ENVIRONMETRICS
*Environmetrics*, **10**, 457–466 (1999)

# DEPOSITION OF WASTE WATER INTO DEEP MINES

PETR PŘIKRYL,[1]* ROBERT ČERNÝ,[2] VLADIMÍR HAVLÍK,[2] KAREL SEGETH,[1]
PETR STUPKA[1] AND JAN TOMAN[2]

[1]*Mathematical Institute of the Academy of Sciences, Žitná 25, CZ-115 67 Prague 1, Czech Republic*
[2]*Faculty of Civil Engineering, Czech Technical University, Thákurova 7, CZ-166 29 Prague 6, Czech Republic*

## SUMMARY

Transport phenomena in contaminated water from waste disposal sites deposited into deep mines are analysed in the paper. Critical transport path for pollutant migration by diffusion of contaminants and buoyancy-driven convection of contaminated water is assumed to be in a vertical cylindrical enclosure. In the first approximation, both transport phenomena are modeled and then numerically simulated separately. The models presented describe ion diffusion and axisymmetric turbulent convection in a vertical cylinder with the radius $R = 3{\cdot}5$ m heated from the sidewalls. One-dimensional diffusion equation is used for simulating the ion diffusion in an enclosure of height $H = 1000$ m. Three low-Reynolds number two-equation turbulence models contained in the FIDAP 7·5 software package were tested in our computational simulations of the natural convection. Two typical case studies of buoyancy-driven convection represent the aspect ratios $H/R = 14{\cdot}3$ and $H/R = 286$. The former corresponds to the initial state just after deposition of the surplus water, the latter to the whole height of the cylindrical enclosure filled by the underground water. The numerical results obtained show that ion diffusion is not dangerous as far as the contamination of subsurface water is concerned. On the other hand, it is concluded that the buoyancy-driven convection in the enclosures with the above aspect ratios can lead to the transport of contaminants into subsurface water and hence the protection of receiving waters from contamination must be designed. 

KEY WORDS ion diffusion; natural convection; transport phenomena; deposition of waste water; computational modeling

## 1. INTRODUCTION

Improvement of the quality of surface and subsurface water resources requires a decrease of pollutants in the aquatic environment. In many countries, deposition of waste products into deep mines is considered to be suitable not only from the economic point of view but also with regard to environmental aspects. For mines which are to be abandoned and rehabilitated, it is advantageous to charge for deposition of some waste products simultaneously with the rehabilitation of the mine. Possible deposition of solid waste such as fly ash waste products from Czech thermal power stations (Vaníček *et al.*, 1995), and/or waste products from nuclear power stations seems to be one of the promising possibilities. However, deposition of contaminated water from waste disposal sites into deep mines has not been resolved yet from geological or from hydrogeological and environmental points of view. The standards for disposing of various waste products such as

* Correspondence to: P. Přikryl, Mathematical Institute of the Academy of Sciences, Žitná 25, CZ-115 67 Prague 1, The Czech Republic.

CCC 1180–4009/99/040457–10$17·50

*Received 12 June 1998*
*Accepted 15 December 1998*

radioactively polluted waters, industrial sludges, fly ash, etc. have become more strict and hence the solution becomes more expensive.

If uranium mining terminates, it is necessary to dispose of waste water from waste disposal sites. There are basically two possibilities how to handle surplus water which was collected in disposal sites of uranium mines: either to use electrodialysis and vaporization or to deposit contaminated water into deep mines. The former possibility would consume a huge amount of energy, the salinity of water would increase and this solution would still require to dispose of solid waste from the process. The latter possibility is less expensive but it requires a complex physico-chemical analysis of transport phenomena and a health risk analysis because the total volume of collected water may be from a half million to one million cubic metres.

## 2. MATHEMATICAL MODELS

Mathematical models have become important tools in solving environmental issues recently, either as research tools to identify gaps in our knowledge, or as operational tools for assessing management strategies to protect the aquatic environment (Abbott *et al.*, 1987; Van der Heide *et al.*, 1988). Hopkirk *et al.* (1981) dealt with coupled convective and conductive heat transfer in the analysis of hot, dry rock geothermal sources. Nobile *et al.* (1989) studied the accuracy of two-equation turbulence modelling in free convection. Ho and Lin (1990) simulated transient thermal convection of two-fluid layers in a horizontal circular enclosure. We describe briefly the models used in our simulations in this section.

### 2.1. Ion transport

Mass diffusion through a region occurs by the motion of quantities of mass or chemical species through the material. A simple model is that in which particles, of local concentration $c$, move through the structure of the material in the direction of decreasing concentration. Such a diffusion mechanism can be described by the diffusion equation (Gebhart 1993)

$$\frac{\partial c}{\partial t} = \mathrm{div}(D\mathrm{grad}c), \tag{1}$$

where $D$ is a material parameter called mass diffusion coefficient or diffusivity. The magnitude of the diffusion coefficient depends strongly on both the material through which diffusion occurs and the diffusing species, $D$ is often also concentration dependent. In a steady state $D$ is uniform across the region of diffusion and in many practical situations may be considered to be constant.

### 2.2. Natural convection

A set of governing equations for two-dimensional buoyancy-driven flows is well known for laminar flow. The equations governing the temperature-driven buoyant flow of a single-phase

 

viscous fluid are mathematical representations of the principles of conservation of momentum, mass and energy. They consist of the following field equations (Launder and Spalding 1974):

$$\operatorname{div} \mathbf{v} = 0, \tag{2}$$

$$\frac{\partial \mathbf{v}}{\partial t} + (\mathbf{v} \cdot \operatorname{grad})\mathbf{v} = \nu \Delta \mathbf{v} - \frac{1}{\rho} \operatorname{grad}(P - P_0) - \beta \mathbf{g}(T - T_0), \tag{3}$$

$$\rho c_P \left( \frac{\partial T}{\partial t} + \mathbf{v} \cdot \operatorname{grad} T \right) = \operatorname{div}(\lambda \operatorname{grad} T). \tag{4}$$

Here, $\mathbf{v}$ is the velocity, $\nu$ is the kinematic viscosity, $\rho$ is the density, $P$ is the pressure, $T$ the temperature ($P_0$ and $T_0$ are the appropriate reference values), $\beta$ is the thermal expansion coefficient, $\mathbf{g}$ the acceleration due to gravity, $C_P$ is the specific heat at constant pressure and $\lambda$ the thermal conductivity of the fluid. The first of the equations is the equation of continuity, then the Navier-Stokes equations in the Boussinesq approximation follow, and the last one is the heat transfer equation.

Flows of practical and industrial relevance are almost always turbulent, which means that the fluid motion is highly random, unsteady and three-dimensional. Due to these complexities, the turbulent motion and the heat-transfer phenomena associated with it are extremely difficult to describe. Nevertheless, it is believed that the solution of the time-dependent three-dimensional governing equations described above can model turbulent flows completely. However, to solve these equations on a computer in the turbulent case is almost impossible even on today's supercomputers. Even they are not fast enough nor do they have the storage capacity to solve these equations directly for the required range of length and time scales. The main reason is that turbulent fluid flow contains scales which are much smaller than the extent of the flow region and the computational mesh to be employed would be far beyond the capabilities of the computer. As a consequence, turbulent motion is modeled in terms of time-averaged quantities today, rather than in terms of instantaneous ones. The criterion for deciding whether laminar or turbulence fluid flow should be expected in our case is the Rayleigh number

$$\mathrm{Ra} = \frac{L^3 \rho^2 g \beta \Delta T c_P}{\nu \lambda}, \tag{5}$$

where $L$ is a characteristic length of the region, $g$ the gravitational acceleration, and $\Delta T$ is a characteristic temperature difference. As a threshold for the transition from the laminar to the turbulent regime, $\mathrm{Ra} = 10^{10}$ is taken mostly.

To develop a practicable turbulent model, the field quantities are divided into their average and fluctuating parts. The steady part is chosen to represent the flow quantities during a time period longer than the smallest events while still allowing gross changes to occur in the flow. Substituting this decomposition into the above field equations and time averaging the terms we arrive to the Reynolds equations of motion (Launder and Spalding 1974), in which, however, additional stress terms called the Reynolds stresses occur. These additional terms represent the temporal mean of the product of the fluctuations about the mean velocity and pressure and, when multiplied by density, they are the additional stresses caused by turbulence in the flow. Turbulence modeling then refers to the process of evaluating these stresses in a feasible manner.

One of the approaches to modeling turbulent stresses introduces the eddy viscosity and evaluates the Reynolds stresses by relating them to the mean velocity gradients, turbulent viscosity,

 

and the turbulent kinetic energy $k$ of the flow, whose dissipation is denoted by $\varepsilon$. The turbulent viscosity is predicted from the solution of additional two semi-empirical transport equations for $k$ and $\varepsilon$. We speak about two-equation models of turbulence in this context. The software package FIDAP used in our numerical simulations of convection includes three most popular two-equation models: the standard $k-\varepsilon$ model of Launder and Spalding (1974), the RNG based $k-\varepsilon$ variant of Yakhot *et al.* (1992) and Wilcox's $k-\omega$ closure (Wilcox 1988).

In our computational model, we employ the penalty method proposed by Temam (1979) and replace the equation of continuity by

$$\varepsilon_P P + \operatorname{div} \mathbf{v} = 0, \tag{6}$$

where $\varepsilon_P$ is the penalty, $\varepsilon_P > 0$, $\varepsilon_P \to 0$. This makes it possible to eliminate the pressure from the remaining equations, and to avoid nearly singular or even singular matrices arising in the discrete analogue of the mass balance equation. Physically, this can be equated to simulating the flow of a very slightly compressible fluid. It is possible to show (Temam 1979) that under certain conditions we can solve the perturbed system in place of the original system without losing any significant accuracy, provided $\varepsilon_P$ is small enough. We note that the pressure variable $P$ is then recovered by post-processing from the velocity field using the perturbed continuity equation (6).

The low Reynolds number $k-\varepsilon$ model has been proposed for turbulence modelling, e.g. by Nobile *et al.* (1989), or for temperature and concentration buoyancy effects by Havlík *et al.* (1995). Numerical simulation of turbulent-free convection for Rayleigh numbers $\mathrm{Ra} > 10^{10}$ is still a challenging problem due to the validity of the $k-\varepsilon$ formulation, the prediction of transition from laminar to turbulent regime and the proper description of turbulence generation and/or dissipation.

## 3. NUMERICAL SIMULATIONS

### 3.1. Ion transport

On the schematic of the underground mines (Figure 1) the dashed area represents deposition of contaminated water from the surface waste disposal site. Typical contaminant concentrations measured in an uranium mine near Příbram (Czech Republic) are as follows: $SO_4^{2-}$ (960–1345 $\mathrm{mgl}^{-1}$), $Cl^-$ (110–674 $\mathrm{mgl}^{-1}$), $U^{238}$ (2·6–3·5 $\mathrm{mgl}^{-1}$) and $Ra^{226}$ (410–618 $\mathrm{mBql}^{-1}$). The lower value corresponds to the raw mine water, the higher one to the contaminated surplus water. Since over the time the lower water layer will be flooded by groundwater from the mining area, the critical path for pollutant migration is assumed to be a vertical cylindrical enclosure (diameter of 7 m).

In the first approximation, ion diffusion and the natural convection can be treated separately. Since the studied case of contaminant transport bears one-dimensional character, a 1-D diffusion equation was used in determining the change of ion concentration in time, namely

$$\frac{\partial c}{\partial t} = D\frac{\partial^2 c}{\partial z^2}, \tag{7}$$

where $c$ is the concentration, $t$ is the time, $z$ is the vertical axis and $D$ is the diffusion coefficient which is assumed to be constant. The particular values of $D$ for our simulations were taken from Incropera and de Witt (1990). The initial and boundary conditions are (see Figure 2) $c(z, 0) \equiv c_1$

 

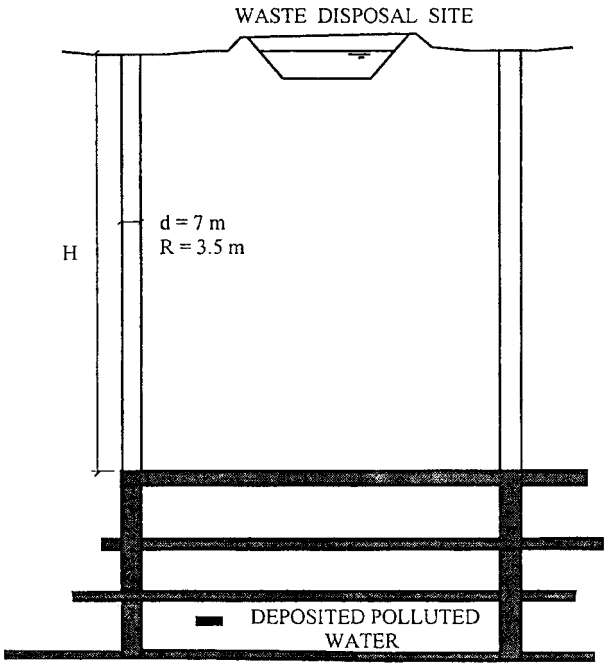


Figure 1. Schematic of the mining area

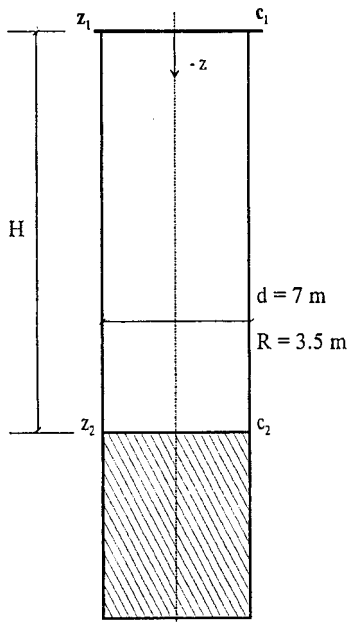


Figure 2. Vertical cylindrical enclosure modeling the shaft of the mine

 

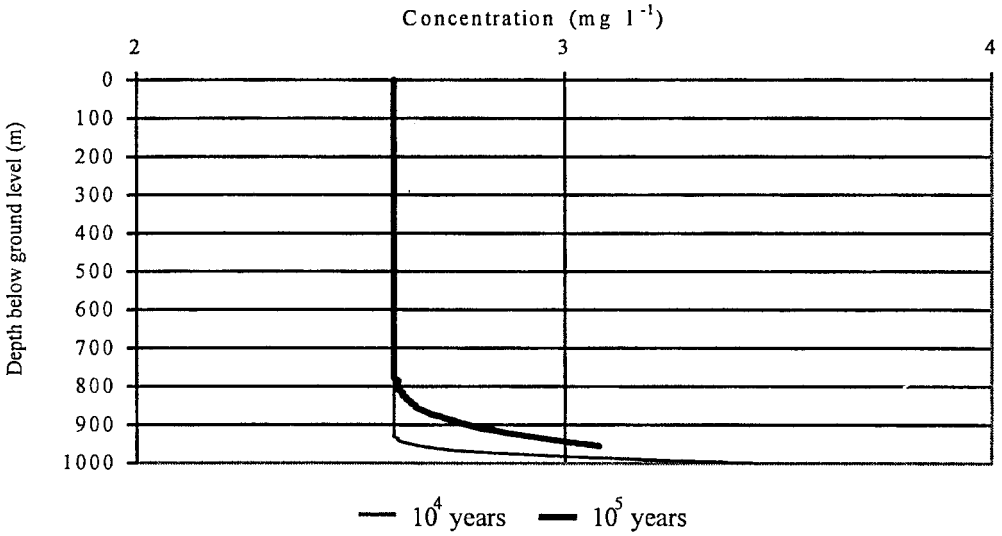


Figure 3. Depth profiles of the concentration of uranium in $10^4$ and $10^5$ years

and $c(z_1, t) = c_1$ and $c(z_2, t) = c_2$, in which $c_1$ and $c_2$ are the ion concentrations in the raw mine water and in the surplus water, respectively. The exact analytical solution can be found in this case (Carslaw and Jaeger 1959) having the form

$$c(x,\ t) = c_1 + (c_2 - c_1)\frac{z - z_1}{z_2 - z_1} + \frac{2}{\pi}\sum_{n=1}^{\infty}\frac{c_2 - c_1}{n}\cos(n\pi)\sin\frac{\pi n(z - z_1)}{z_2 - z_1}\ \exp\left(-\frac{Dn^2\pi^2 t}{(z_2 - z_1)^2}\right). \quad (8)$$

Figures 3–5 show examples of calculated values of ion concentration for uranium and selected ions for $z_1 = 0$ m and $z_2 = 1000$ m, which are assumed to be typical values for the type of mines under consideration. It is apparent that even after $10^5$ years the ions cannot achieve the ground level and contaminate the surface water.

### 3.2. Simulation of natural convection

We simulated selected characteristic cases of natural convection in a vertical enclosure modeling a uranium mine, which was identified as the critical path for pollutant migration. The modeled cases describe axisymmetric convection in a vertical cylinder with the diameter $d = 7$ m, which is heated from the sidewalls. Due to cylindrical symmetry it was possible to perform the computations with a 2-D model. Axial symmetry allows us to consider only the left half of the enclosure. Two typical case studies were selected. In Case 1, the aspect ratio $H/R = 14{\cdot}3$ corresponds to the initial state just after deposition of the surplus water. In Case 2, the aspect ratio $H/R = 286$ represents the whole height of the cylindrical enclosure, i.e. the final state after filling the enclosure by the underground water. A constant temperature gradient in the vertical direction was assumed, $-0{\cdot}026$ K m$^{-1}$. In the numerical simulations, the steady flow in the system was calculated.

The material parameters were measured using the samples of contaminated water from the waste disposal site Bytíz near Příbram (Czech Republic). Dynamic viscosity was

 

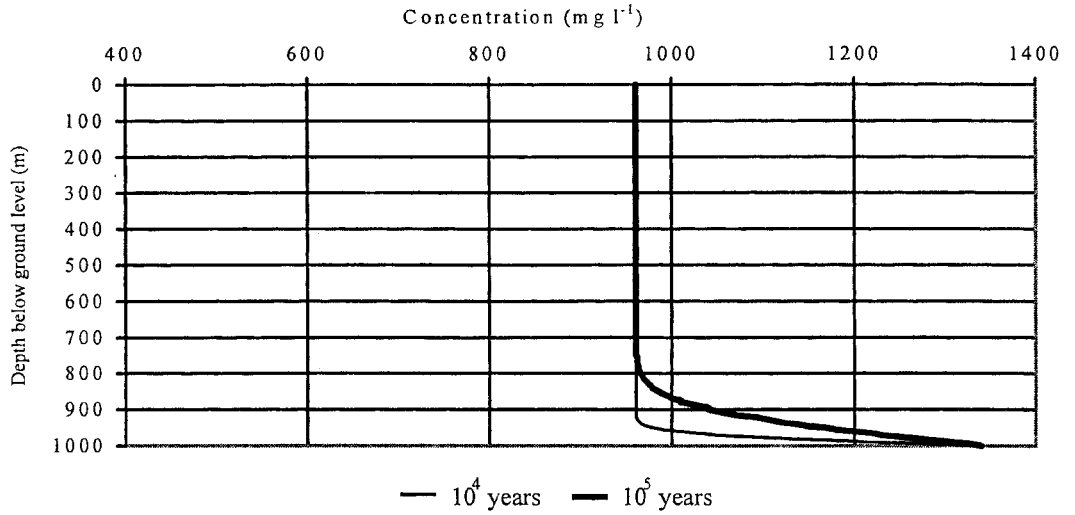


Figure 4. Depth profiles of the concentration of $SO_4^{2-}$ ions in $10^4$ and $10^5$ years

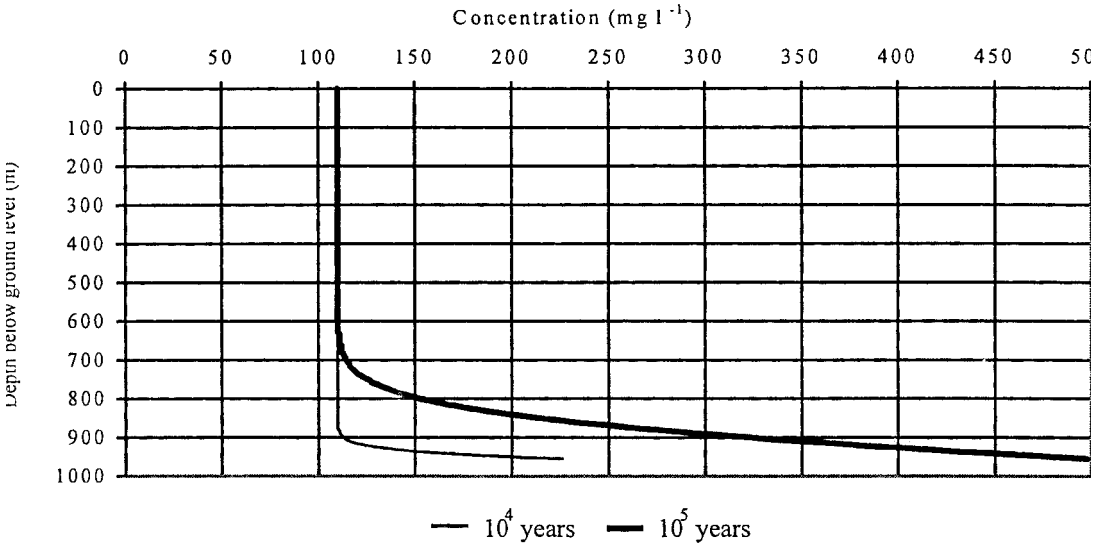


Figure 5. Depth profiles of the concentration of $Cl^-$ ions in $10^4$ and $10^5$ years

$0{\cdot}91 \times 10{\cdot}3$ kg m$^{-1}$ s$^{-1}$, thermal conductivity 0·6 W m$^{-1}$ K$^{-1}$ and the density 1002·7 kg m$^{-3}$. The measured temperature-induced variations of volume thermal expansion coefficient which affects the buoyancy forces in the enclosure significantly was in the temperature range from 15 to 25°C equal to $3{\cdot}3 \times 10^{-4}$ K$^{-1}$ on the average.

In the numerical studies FIDAP 7·5 computer code was employed, which is remarkably improved as for the turbulence models compared to version 7·0 used in our previous numerical studies (Černý *et al.* 1996). First, we modeled Case 1 with the aspect ratio $H/R = 14{\cdot}3$. The Rayleigh number was based on the radius of the vertical cylinder and in both cases was as high as

 

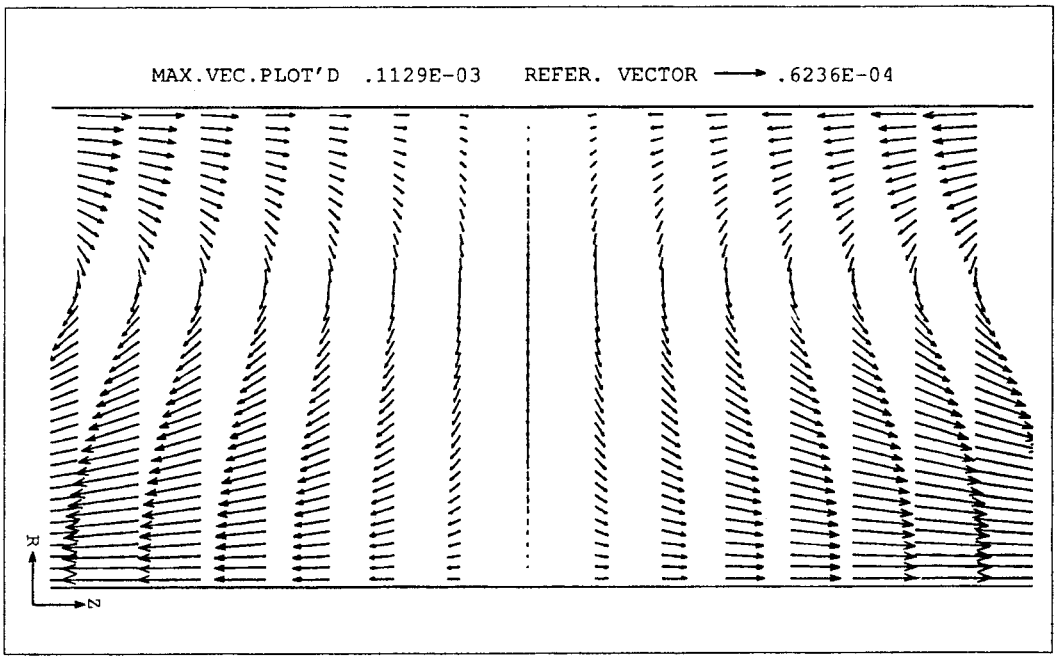


Figure 6. Velocity vector field in Case 1; a section of the central part; $k-\omega$ model

$10^{12}$. Therefore, no stable steady-state laminar solutions should be expected. We tried to perform the numerical experiments with the laminar approximation anyway because the results could provide a safe upper limit for estimating the velocity magnitude compared to the more correct turbulence models, if the solution converged. In addition, we have tested three turbulence models, namely the classical $k-\varepsilon$ model, the RNG model and the low-Reynolds number $k-\omega$ model (see FIDAP 7·5 Documentation 1995).

A set of numerical calculations was performed in order to optimize the numerical parameters of the model, namely the number of finite elements, the type of iteration procedure, and the magnitude of the pressure penalty $\varepsilon_P$, to obtain acceptable accuracy in an affordable CPU time. The following optimum values were obtained: $200 \times 50$ finite elements mesh, combined iteration procedure consisting of one successive approximation and then Newton-Raphson method, the pressure penalty $\varepsilon_P = 10^{-10}$. Particularly the pressure penalty had a remarkable influence on the accuracy of results because no convergence to a steady-state solution was achieved for any penalties outside the interval $10^{-11}$ to $10^{-10}$.

In the calculations, the laminar approximation of the steady-state solution has converged very fast in spite of the very high Rayleigh number. Only three iterations were necessary to obtain relative accuracy in the velocities as good as $10^{-6}$. Both the $k-\varepsilon$ and RNG models failed to converge in modeling the turbulent steady-state solution, but the low-Reynolds number $k-\omega$ model converged very fast. Again, only three iterations were necessary to obtain a $10^{-6}$ accuracy in velocities. Both laminar and turbulent solutions obtained in our calculations had a very similar velocity pattern. The typical magnitude of velocities for the turbulent $k-\omega$ model was by one or two orders of magnitude lower as compared with the laminar model. From Figure 6, which

 

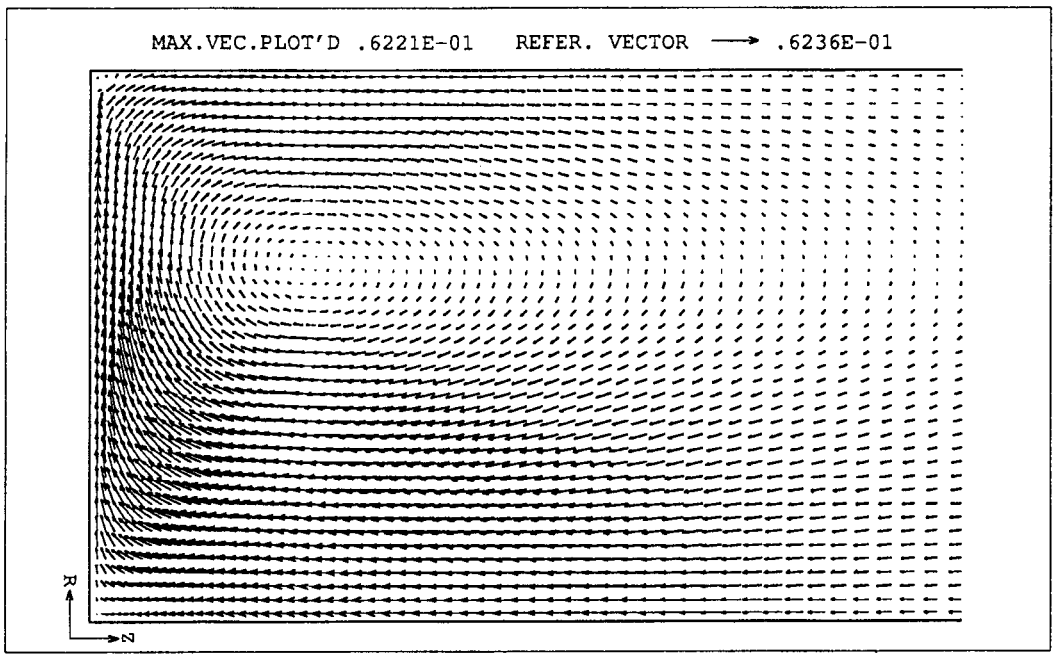


Figure 7. Velocity vector field in Case 1; a section of the lower part; $k-\omega$ model

displays a section of the central part of the enclosure, two recirculating flow regions are apparent. Figure 7 illustrates the lower part of the enclosure.

In Case 2 (aspect ratio $H/R = 286$), converged steady-state solutions were obtained for both laminar approximations and the $k-\omega$ turbulent model as in Case 1, but the character of the solutions was slightly different. We observed two separate recirculating flow regions at the upper and lower ends of the enclosure which were separated by almost zero-velocity flow in the middle part. Since the flow in this middle part was in the upward direction only, the calculated flow pattern was not realistic. It should be noted that similar unrealistic flow in the middle part of the enclosure was also obtained in Case 1 when the pressure penalty was too high, typically $10^{-6}$. We have thus tried to perform the optimization of the pressure penalty value again, but optimum pressure penalty was not found in this case because decreasing the value of $\varepsilon_P$ led to numerical instabilities.

For the sake of comparison, the calculations with the aspect ratio $H/R = 1$ were also done. The structure of the flow was very similar to Case 1 with $H/R = 14{\cdot}3$. Again, both the laminar approximation and the $k-\omega$ model led to two recirculating flow regions, even the magnitudes of the velocities were similar. The $k-\varepsilon$ model and RNG model did not achieve any converged steady-state solution.

## 4. CONCLUSIONS

Transport processes in the contaminated water, which is planned to be deposited into a deep uranium mine near Příbram, were situated numerically. It can be concluded that the ion diffusion itself cannot cause contamination of subsurface water even after $10^5$ years. For both laminar and

 

turbulent natural convection, two recirculating flow regions were obtained. Hence, it could be believed that the pollution would not impact the subsurface water in the upper half of the enclosure. However, the interaction between these two flow regions must be taken into account, which is impossible with the two-equations models of turbulence based on time-averaged quantities. One of the possible approaches which could lead to adequate modeling of turbulent fluctuations in the contact region in the central part of the enclosure would be direct numerical simulation (DNS) of turbulence based on the original system of governing equations. As we noticed in Section 2·2, this is impractical for most computer facilities at this moment.

The theoretical results together with the health risk analysis can help the engineers to design a final project of disposing of surplus water from the waste disposal site. Our results imply that the construction of a Waste Water Treatment Works for the treatment of contaminated water from the mining area is necessary in order to protect the environment from pollution.

ACKNOWLEDGEMENT

The research reported here has been supported by the Grant Agency of the Czech Republic Grant #103/96/1710.

## REFERENCES

Abbott, M. B. *et al*. (1987). 'An introduction to the European Hydrological System, SHE, 2: Structure of a physically-based, distributed modelling system'. *Journal of Hydrology* **87**, 61–77.

Carslaw, H. S. and Jaeger, J. C. (1959). *Conduction of Heat in Solids*. Oxford: Clarendon Press.

Černý, R., Havlík, V. and Sklenář, P. (1996). 'Numerical simulation of a natural convection'. In *Workshop 96*. VUT Brno, 353–354.

*FIDAP 7.5 Documentation* (1995). Lebanon, NH, Fluent Inc..

Gebhart, B. (1993). *Heat Conduction and Mass Diffusion*. New York: McGraw-Hill.

Havlík, V., Černý, R., Hrstka, O., Toman, J. and Přikryl, P. (1995). 'Temperature driven natural convection in a vertical enclosure'. *HYDRA 2000. Proceedings of the XXVIth Congress of the IAHR, Part 2*, ed. M. A. Leschziner. London: Thomas Telford, 70–75.

Ho, C. J. and Lin, Y. H. (1990). 'On simulation of transient thermal convection of two-fluid layers in a horizontal circular enclosure'. *International Journal of Heat and Fluid Flow* **11**, 355–361.

Hopkirk, R. J. *et al*. (1981). 'Coupled convective and conductive heat transfer in the analysis of hot, dry rock geothermal sources'. In *Numerical Methods in Heat Transfer*, eds. R. W. Lewis, K. Morgan and O. C. Zienkiewicz. New York: John Wiley, 261–303.

Incropera, F. P. and de Witt, D. P. (1990). *Fundamentals of Heat and Mass Transfer*. New York: John Wiley.

Launder, B. E. and Spalding, D. B. (1974). 'The numerical computation of turbulent flows'. *Computational Methods in Applied Mechanics and Engineering* **3**, 269–289.

Nobile, E., Sousa, A. C. M. and Barozzi, G. S. (1989). 'Accuracy of two-equation turbulence modelling in free convection'. *Numerical Methods in Thermal Problems*, Vol. VI, eds. R. W. Lewis and K. Morgan. Swansea: Pineridge Press.

Temam, R. (1979). *Navier-Stokes Equations*. Amsterdam: North-Holland.

Van der Heijde, P. K. M. and Prickett, A. (1988). 'Groundwater-quality models for planning, management and regulation'. In *Proceedings of the International Symposium on Water Quality Modelling of Agricultural Non-point Sources, Part 1*. Logam, Utah, 279–306.

Vaníček *et al*. (1995). *Depositing Solid Waste Products into Underground Cavities*. Prague: Czech Technical University Report GA 118/93 (in Czech).

Wilcox, D. C. (1988). 'Reassessment of the scale determining equation for advanced turbulence models'. *AIAA Journal* **26**, 1299–1310.

Yakhot, V., Orszag, S. A., Thangam, S., Gatski, T. B. and Speziale, C. G. (1992). 'Development of turbulence models for shear flows by a double expansion technique'. *Physics of Fluids A* **4**, 1510–1520.

 